Scientia Iranica A (2020) 27(3), 1019–1027

Sharif University of Technology
Scientia Iranica
Transactions A: Civil Engineering
http://scientiairanica.sharif.edu

Effects of content and thickness on the microstructure as well as optical and electrical properties of oxidized Al-doped ZnO films

S. Liu[a,b], G. Li[a,c,*], L. Xiao[a,b], B. Jia[a,c], Z. Xu[a,c], and Q. Wang[a,c]

a. *Key Laboratory of Electromagnetic Processing of Materials (Ministry of Education), Northeastern University, Shenyang 110819, China.*
b. *School of Materials Science and Engineering, Northeastern University, Shenyang 110819, China.*
c. *School of Metallurgy, Northeastern University, Shenyang 110819, China.*

Received 18 April 2017; received in revised form 12 December 2017; accepted 2 July 2018

KEYWORDS
ZnO film;
Oxidation growth;
Vacuum evaporation;
Transparent electrode.

Abstract. Controlling conductivity and optical transmittance of Al-doped ZnO (AZO) thin films in the application of optoelectronic materials is a crucial requirement. In this study, AZO thin films were prepared by oxidizing thermally evaporated Zn-Al thin films in open air. Then, the effects of Al contents and film thicknesses on the microstructure and optical and electrical properties of the AZO films were studied. The results showed that the optical and electrical properties of the AZO films were affected by Al content and change in thickness. The Haacke figure of merit reached 2.91×10^{-4} Ω^{-1} and film surface morphology changed by Al content. Nanowire was formed when Al content was 9.58%. The Al_2O_3 phase appeared with an excessive Al content. Transmittance of the AZO films was less than 25% when Al content was more than 9.58%. Grain size first increased and then, decreased with increase in film thickness when Al content remained at 2%. Within the limits of the available transmittance, sheet resistance and transmittance of the AZO thin film decreased exponentially with increase in film thickness.

1. Introduction

Transparent electrode is one of the most important components of optoelectronic devices and has extensive application in solar cells, displaying, and sensors [1]. The transparency of semiconductors is dependent on band gap [2]. Zinc oxide (ZnO) has a wide band gap (3.37 eV) and possesses high transmittance in the range of visible light [3]. Thus, ZnO thin films can also be used as an eco-friendly buffer layer in photovoltaic application. Furthermore, their optical properties can be affected by thermal annealing temperature for recrystallization. This leads to a transmission over 70% in the visible region [4]. Doping element in ZnO can enhance electrical conductivity without reducing transmittance. This is an effective method to fabricate transparent electrodes. Among various dopants, Al is one of the most popular ones due to its abundance and low cost. In addition, Al element doped in ZnO is a promising way of producing transparent electrodes, because Al dopant increases electrical conductivity and

*. *Corresponding author.*
E-mail addresses: liu_shiying0907@sina.com (S. Liu); ggli@epm.neu.edu.cn (G. Li); 3998147520@136.com (L. Xiao); jia_baohai@163.com (B. Jia); a2765527751@qq.com (Z. Xu); wangq@epm.neu.edu.cn (Q. Wang)

doi: 10.24200/sci.2018.20644

meanwhile, leads to a blue shift of optical absorption edge [5]. The conductivity of the Al-doped ZnO (AZO) transparent conductive films is similar to that of ITO [6]. Furthermore, the stability of the AZO film, e.g. in plasma, is higher than that of the ITO film. Thus, AZO is one of the best substitutions for ITO.

The optical and electrical properties mainly depend on the composition, thickness, and content of the AZO films. Increase in Al content can reduce the transmittance due to the opaqueness of aluminum. Also, increase in thickness decreases transmittance [7]. Additionally, transmittance is dependent on microstructure and band gap. The scattering of impurity defects has a significant influence on light transmittance [8]. Ordered structure reduces light scattering and enhances transmittance by impurity and the dopant [9]. On the other hand, increase in carrier concentration and mobility is important to improve conductivity of the AZO films. Conductivity can be improved by increasing dopant content, because carrier concentration is close to the doping amount with a small dopant. In addition, conductivity is improved by increasing migration channel via forming nanowires [10–12]. The above facts imply that thickness, dopant content, and morphology play a key role in enhancing the performance of transparent electrodes. However, they have direct influence on each other. For example, increase in thickness can improve grain size, resulting in the change of conductivity and decrease in transmittance [13–15]. The Al content tunes carrier concentration and electrical properties and leads to different surface morphologies [16,17]. Thus, it is very important to study the effects of Al content and thickness on the microstructure and optical and electrical properties of the AZO films in application.

Many methods have been adopted to fabricate the AZO films such as magnetron sputtering, pulsed laser deposition, molecular beam epitaxy, sol-gel, and hydrothermal synthesis [18]. Sog-gel method is a simple way of preparing ZnO without the need for vacuum. The impurity content can be suppressed by annealing at proper temperature [19]. Magnetron sputtering has the quality of high growth rate, uniform surface, and high cohesion. The resistivity of the AZO film fabricated by this method can reach 1×10^{-4} Ω.cm. Film quality is influenced by substrate temperature, sputtering power, gas pressure, and target composition [20,21]. Pulsed laser deposition is a film forming method that creates accurate composition and smooth surface and can fabricate multiple layers at a low substrate temperature [22]. However, in the above-mentioned methods, it is difficult to accurately tune thickness, composition, and morphology at the same time. Recently, ZnO films with various dopants have been fabricated by oxidizing metallic Zn films evaporated in vacuum [23,24]. The metallic Zn films have high purity and low defect because of the vacuum condition. Surface morphology can be changed by the oxidation temperature and duration time.

In this study, AZO films were fabricated by oxidizing the as-deposited Zn-Al films in open air. The Zn-Al films were prepared by co-evaporating Zn and Al. Al content was controlled by changing the Al source temperature. Thickness varied by deposition time. Then, the as-deposited Zn-Al films were oxidized at 600°C for 1 hour in open air. In AZO films, the effects of Al content and thickness on the microstructure and optical and electrical properties were explored. Haacke figure of merit ($\varphi = T^{10}/R_{sheet}$, T is transmittance and R_{sheet} is sheet resistivity) was used to appraise the performance of the films [25].

2. Experimental details

AZO films were fabricated in two steps. First, the Zn-Al films with different Al contents and film thicknesses were prepared by changing Al source temperature and deposition time in thermal vacuum evaporation equipment [26]. High purity materials of Zn particles (99.999%) and Al particles (99.999%) with a diameter of about 3 mm were selected as the source materials. The substrates were polished quartz plates. Transmittance was about 93%. Substrate temperature was ambient. The base pressure of the chamber was better than 8.0×10^{-5} Pa and the work pressure was about 1.2×10^{-4} Pa. Second, the AZO was obtained by oxidizing the above-mentioned Zn-Al films at 600°C for 1 hour in furnace in open air.

Surface morphology of the films was observed by Scanning Electron Microscopy (SEM; SUPRA 35, Carl Zeiss Inc., Oberkochen, Germany). The Al content was determined by Energy Dispersive X-ray Spectroscopy (EDS; Inca, Oxford). The thicknesses were measured by using Atomic Force Microscopy (AFM, Nanosurf, Flex-Axiom C3000, Switzerland). The crystal structure of the films was examined by X-Ray Diffraction (XRD, DMAX 2400, Rigaku) with a grazing incidence of 2° in $\theta - 2\theta$ mode with monochromatic Cu $K_{\alpha 1}$ radiation ($\lambda = 0.154056$ nm). Optical transmittance was measured by a UV-vis spectrophotometer (Lambda 750S, PerkinElmer). Sheet resistivity was measured via the four-probe method.

3. Results and discussion

3.1. Effect of Al content on the microstructure and properties of the AZO films

The as-deposited Zn-Al films with the thickness of about 500 nm were achieved by changing the Al source temperature. The EDS results indicated that Al contents in the as-deposited films were 4.44%, 10.55%, 15.81%, and 61.01%. Also, Al contents in

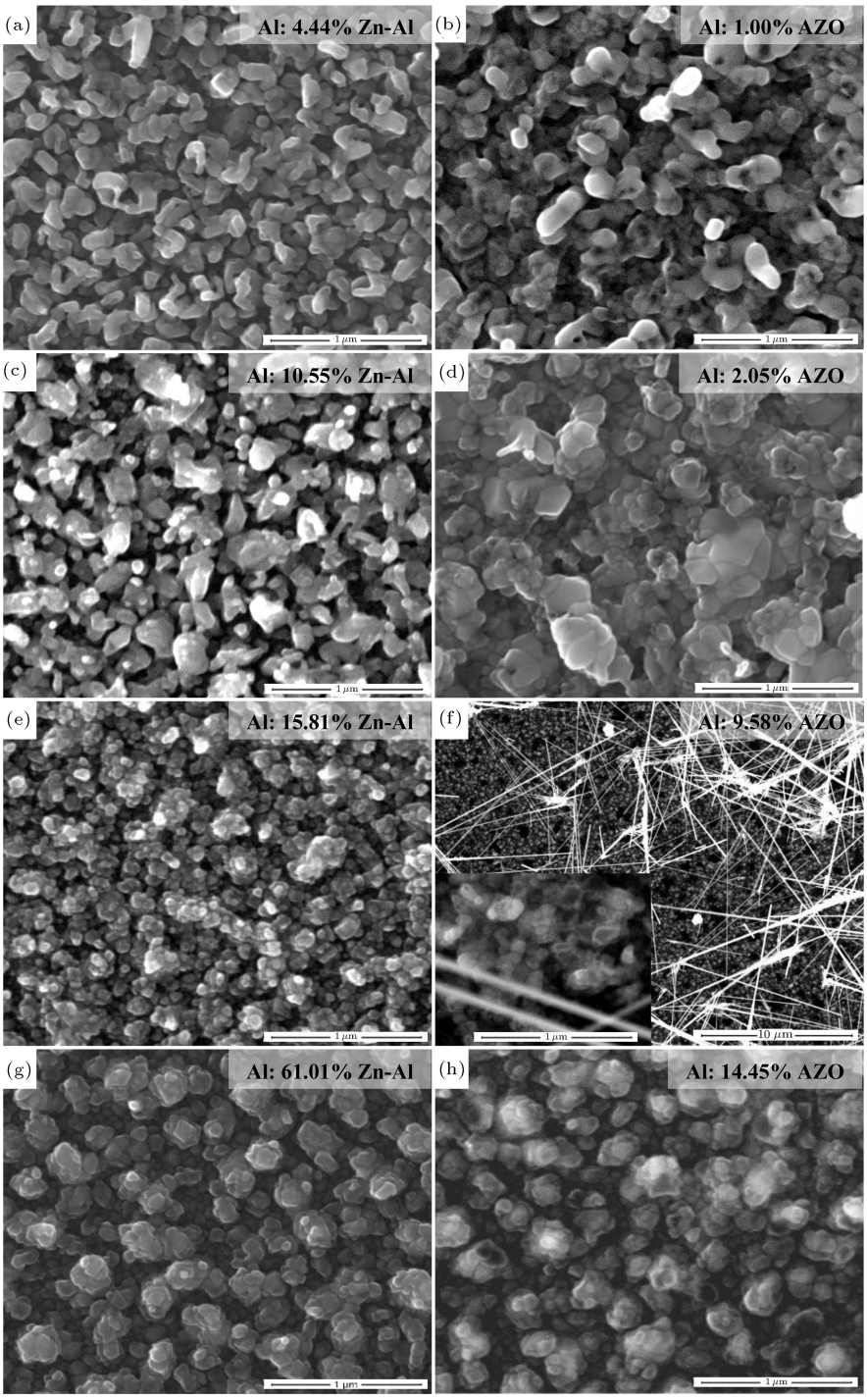

Figure 1. SEM images of the as-deposited Zn-Al films (left column) and the AZO films (right column).

the AZO films were 1.00%, 2.05%, 9.58%, and 14.45% after the films oxidized. Figure 1 shows the SEM images of the as-deposited Zn-Al and AZO films with different Al contents. It can be seen that the surface morphologies are strongly related to the Al contents. Grain sizes on the surface increased after oxidation. When Al content was low, the grain had small size with column structure, as shown in Figure 1(a). The grain was aggregated after oxidation, which made the film become dense, as shown in Figure 1(b). The surface grain grew like a column perpendicular to the substrate with the Al content increasing. The perpendicular column became an island after oxidation, as shown in Figure 1(c) and (d). When the Al content in the AZO film increased to 9.58%, the surface grains were refined. Nanowires appeared on the surface after oxidation. However, the bottom was still formed by small grains. This is because particles protruding from the surface

form a nanowire structure in the oxidation process. The average length of the nanowires was about 10 μm. When the Al content in the AZO film was 14.45%, the grain sizes increased and the grains were significantly aggregated. After oxidation, no nanowire and many islands appeared in the film because Al content was high and suppressed the growth of nanowires. These results indicate that Al content has a significant effect on the surface morphology. Al content can be adjusted to tune the grain size and formation of particles, island, and nanowire.

XRD patterns of the as-deposited Zn-Al films with different Al contents are shown in Figure 2(a). Clearly, only Zn peaks exist and no Al peaks appear when Al content is lower than 10.55%. It also can be seen that the positions of Zn (102) peak shift to 56.28° from 54.6°. This means that Al atoms are doped in the Zn lattice. As a result, only Zn phase exists when Al content is low. In addition, the atomic radius of Al (0.143 nm) is higher than that of Zn (0.134 nm). Thus, an increase in Al content enhances the lattice constant and improves inter-planar spacing. The Al atoms cannot be doped into the Zn lattice adequately when Al content increases ($\geq$ 15.81%). Therefore, the (200) and (220) peaks of Al phase appear.

The XRD patterns of the AZO films with different Al contents are shown in Figure 2(b). Only hexagonal wurtzite ZnO phase existed in the AZO films when the Al contents were 1.00% and 2.05%. When Al content was low, Al^{3+} substituted Zn^{2+} in the wurtzite lattice or occupied the interstitial site in the ZnO lattice. Moreover, in comparison with the standard card (JCPDS no. 36–1451) of hexagonal wurtzite ZnO phase, the XRD peaks of the AZO films shifted to a high 2θ. This means that the Zn ion with a large radius (0.074 nm) was substituted by the Al ion with a small radius (0.054 nm). This resulted in the reduction in ZnO lattice constant [27]. When Al content was 9.58%, ZnO (002) peak disappeared. The (113) and (116) peaks of Al_2O_3 phase appeared in the XRD pattern. That is, two phases of ZnO and Al_2O_3 coexisted in the film.

Furthermore, the existence of Al_2O_3 inhibits the (002) growth of ZnO [28]. When Al content was 14.45%, the (100), (002), and (102) peaks of ZnO disappeared and the (111) peak of Al appeared. This means that the film was mainly formed by Al_2O_3 and a small amount of ZnO and Al phases. This illustrates that a large amount of Al cannot be doped into ZnO lattice to form Al_2O_3 phase and it forms pure Al phase. These results lead to the conclusion that Al content is one of the most important factors in controlling the phase formation of the AZO films. A small amount of Al can modify the lattice constant of ZnO and a large amount of Al will inhibit the formation ZnO and becomes insulated Al_2O_3.

The transmittance of the AZO films with different Al contents was measured, as shown in Figure 3. The results indicated that the transmittance for visible and infrared light in the wavelength range of 400–2000 nm decreased with increase in Al content. According to the XRD results, it was found that transmittance was reduced to below 50% when the Al_2O_3 phase appeared at 9.58% Al. This means that the appearance of Al_2O_3 reduced transmittance. In addition, the transmittance for the ultraviolet light (300–400 nm) of the film with 9.58% Al was much higher than those with other Al contents. This is because the formation of nanowires makes the ultraviolet absorption edge shift to the short wavelength [29].

Sheet resistivity is measured by four-probe method. Resistivity is calculated by multiplying sheet

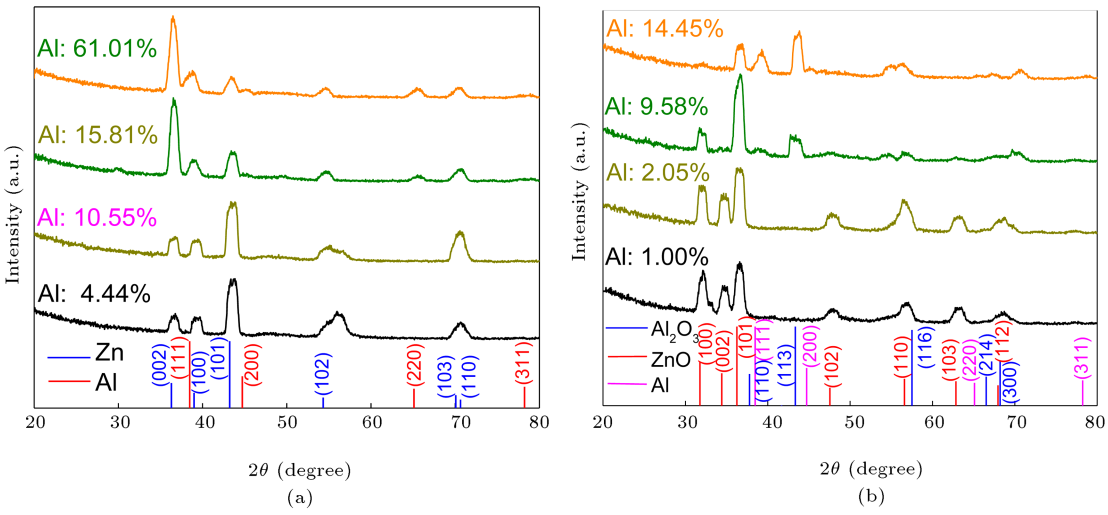

Figure 2. XRD patterns of the as-deposited Zn-Al films (a) and AZO films (b) with different Al contents. The standard peaks of Zn, Al, ZnO, and Al_2O_3 are also shown.

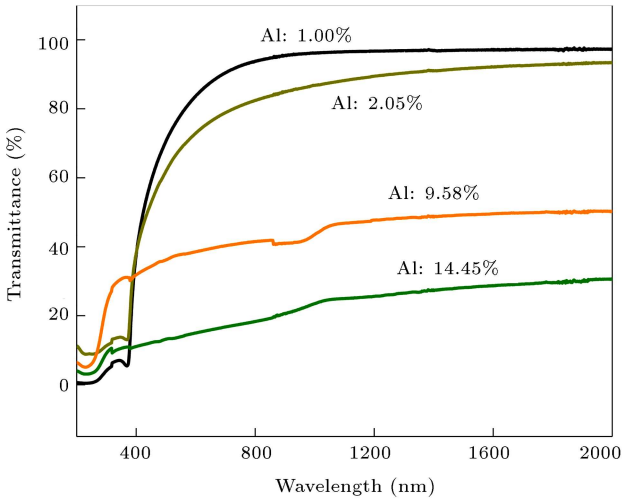

Figure 3. Transmittance spectra of the AZO films with different Al contents.

Table 1. Relationship of transmittance, sheet resistivity, and resistivity of the AZO thin films with Al content.

Al content (%)	1.00	2.05	9.58	14.45
Transmittance (%)	85.31	75.4	24.97	17.42
Sheet resistivity ($\Omega.cm^{-2}$)	1141	2050	1800	298
Resistivity ($\Omega.cm$)	0.057	0.103	0.09	0.015

resistivity by thickness. The results are shown in Table 1. The relationships between transmittance and sheet resistivity in AZO films with Al contents are identified as shown in Figure 4. It can be seen that sheet resistivity decreases with increase in Al content. It decreases sharply when the Al phase appears in the AZO film with 14.45% Al. Also, transmittance is reduced significantly. The transparent electrode requires the transmittance to be in the range of 75%–95% and the sheet resistivity to be in the range of

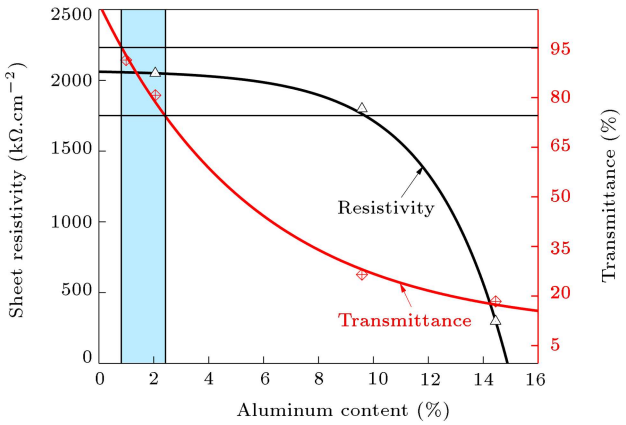

Figure 4. Relationship between transmittance and sheet resistivity of the AZO thin films as a function of Al content.

$10^0 - 10^5$ $\Omega.cm^{-2}$ [30]. Thus, the films could meet the requirements of transparent electrode when Al content was lower than 2.4%. At this point, sheet resistivity was about 2050 $\Omega.cm^{-2}$. Transmittance decreased with decreasing Al content. The maximum value of the Haacke figure of merit reached 2.91×10^{-4} Ω^{-1}.

3.2. *Effect of thicknesses on the microstructure and properties of AZO films*

Thickness plays a key role in determining transmittance when Al content remains unchanged. With 2% Al content, thicknesses of the AZO films were 50, 200, 500, and 800 nm. Their SEM images are shown in Figure 5. When thickness was 50 nm, the surface grain size was below 50 nm distributed uniformly. The grain shape was spherical and the size experienced a small increase after oxidation. Grain size was about 150 nm and particle boundaries disappeared at the thickness of 200 nm. In the 500 nm film, the as-deposited particle grew perpendicular to the substrate. Some small particles existed in the column. The island structure appeared after oxidation. The column obviously grew perpendicular to the substrate when film thickness was 800 nm. However, grain size was reduced and the small grain size led to the uniform distribution of particles in the AZO film. No island like that in the case of 500 nm appeared. These results indicated that the surface morphologies were strongly affected by the thickness.

XRD patterns were used to analyze phase formation of the AZO films with different thicknesses, as shown in Figure 6. It can be seen that the positions of appearing peaks are identical in all the AZO films. Only the hexagonal wurtzite ZnO phase existed in these films. This means that phase formation was not influenced by thickness. The main difference was in the intensity of the peaks. Intensity increased with increase in thickness and the strong intensity indicated the improvement of crystallinity. Meanwhile, the FWHM of (002) peak decreased with increase in thickness. This proves that grain size increases with increase in thickness [14,31].

Transmittance of the AZO films with different thicknesses is shown in Figure 7. Transmittance of the visible and infrared light was reduced with thickness increasing. The ultraviolet absorption edge slightly shifted to red with increase in thickness. Film transmittance with the thicknesses of 200, 400, 500, 600, and 800 nm was 93.46%, 78.75%, 75.4%, 57.45%, and 54.08%, respectively, in the visible light range. In addition, it was found that the effect of Al content on transmittance was much stronger than that of thickness. The 50 and 200 nm films were too thin to achieve sheet resistivity by the four-probe method. Sheet resistivity of the films with 400 and 500 nm was respectively 4100 and 2050 $\Omega.cm^{-2}$ and the films

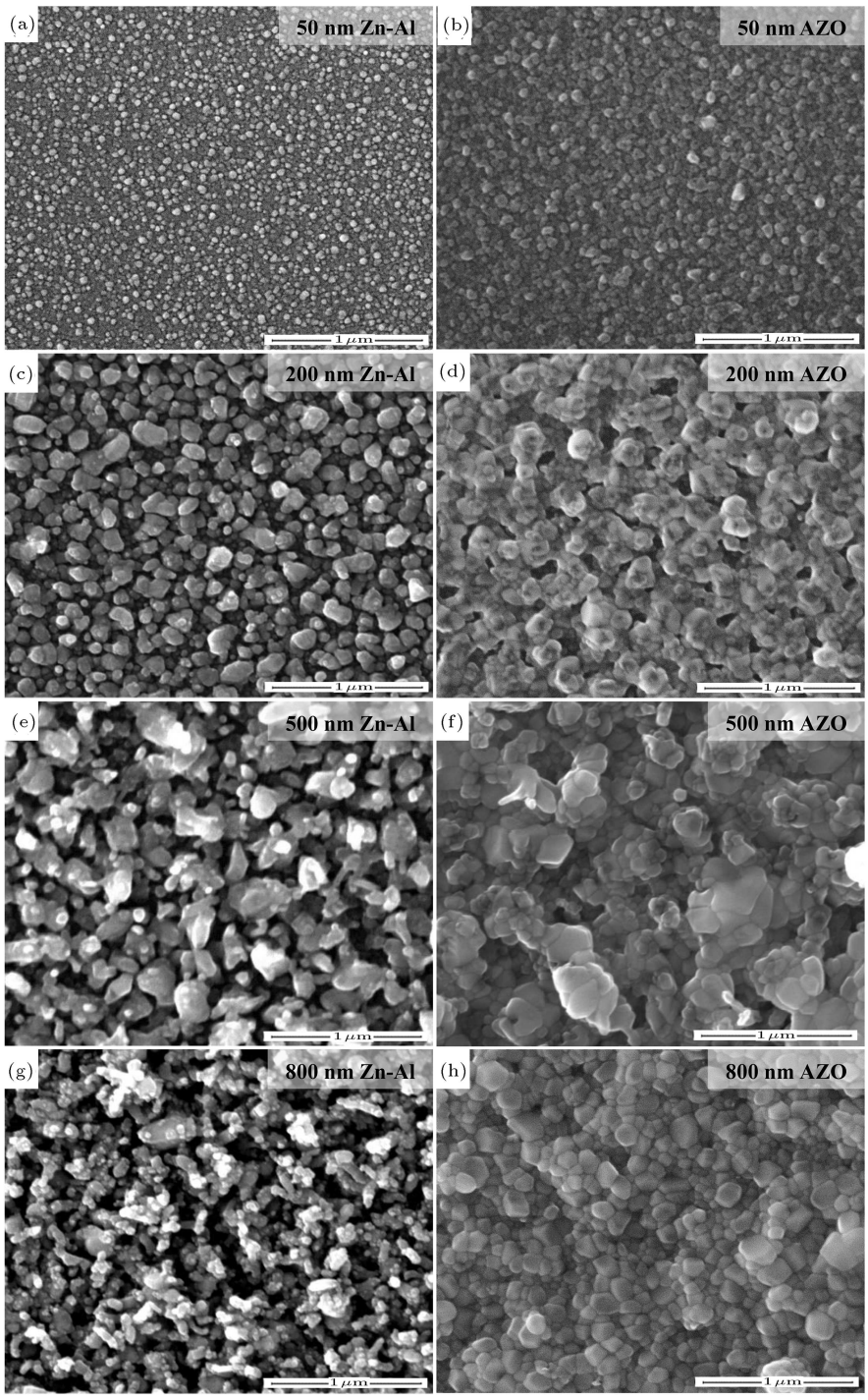

Figure 5. SEM images of the as-deposited Zn-Al and the AZO films with different thicknesses.

with 600 and 800 nm was respectively 641.6 and 523.4 $\Omega.cm^{-2}$.

In the same way as shown in Figure 4, the relationships between transmittance and sheet resistivity in the AZO thin films with different thicknesses are illustrated in Figure 8. Sheet resistivity and transmittance were reduced with increase in thickness. Sheet resistivity decreased exponentially with increasing film thickness. Thickness in the blue zone could meet the demands of transparent electrode. The Haacke figure of merit of the film was non-monotonic with thickness. The maximum value was 1.44×10^{-5} Ω^{-1} when the thickness was 457 nm.

In summary, Al content should be maintained at less than 2.4% in order to meet the requirement of transmittance of 75%–95%. In this case, sheet resistivity is stable about 2050 $\Omega.cm^{-2}$. Increase in doping content significantly reduces the transmittance

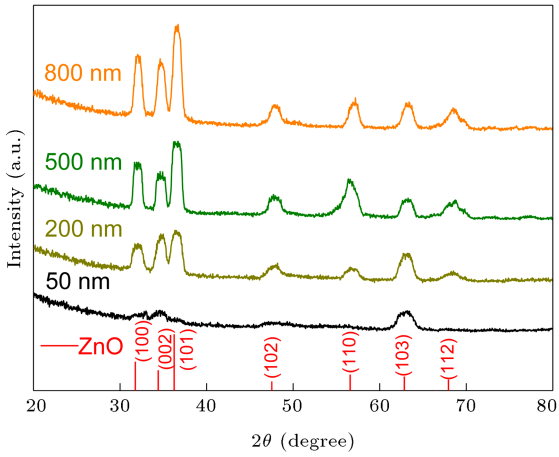

Figure 6. XRD patterns of the AZO films with different thicknesses.

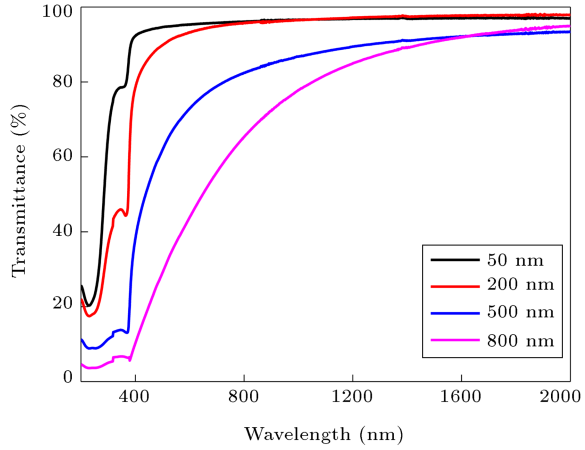

Figure 7. Transmittance spectra of the AZO films with different thicknesses.

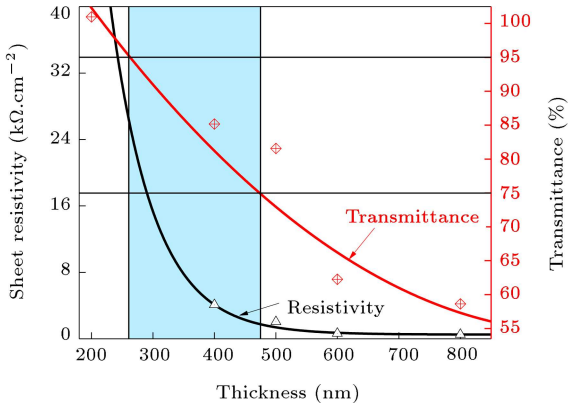

Figure 8. Relationship between transmittance and sheet resistivity of the AZO thin films as a function of thickness.

of the AZO film and hence, the Haacke figure of merit. When Al content is about 2%, thickness in the range of 260–480 nm would meet the requirement of transmittance. In this thickness range, the film is formed by island particle. Sheet resistivity and transmittance decrease exponentially with increase in film thickness. Moreover, the Haacke figure of merit of the film is non-monotonic with thickness. Thus, Al content and thickness can be adjusted to accurately tune the Haacke figure of merit. The optical and electrical properties can meet the demands of transparent electrode by oxidation of the evaporated Zn-Al films.

4. Conclusions

In this study, AZO films were obtained by oxidizing evaporated Zn-Al films in thermal vacuum in open air. The effects of Al content and thickness on the microstructure, transmittance, and resistivity were explored. The results showed that Al content changed grain size and surface morphology. Nanowires appeared when Al content was 9.58%. The Al_2O_3 phase suppressed the growth of (002) peak of ZnO. When Al content was 2%, only hexagonal wurtzite ZnO phase formed with the thickness of 50-800 nm. Increase in Al content and thickness reduced transmittance; however, the former was much more significant than the latter. Thus, in order to meet the demands of the transparent electrode, Al content was kept at less than 2.4% and thickness was 457 nm. In this circumstance, the Haccke figure of merit reached $2.91 \times 10^{-4}\ \Omega^{-1}$. This means that the thermal oxidation method of evaporated Zn-Al films can be used to fabricate AZO transparent electrodes.

Acknowledgements

The authors would like to acknowledge the financial support of National Natural Science Foundation of China (Grant Nos. 51906033 and 51690161), and the Fundamental Research Funds for the Central Universities (Grant Nos. N2025016, N180902011 and N170908001) and Youth Science and Technology Innovation Talents of Shenyang (Grant No. RC190441).

References

1. Nomura, K., Ohta, H., Ueda, K., Kamiya, T., Hirano, M., and Hosono, H. "Thin-film transistor fabricated in single-crystalline transparent oxide semiconductor", *Science*, **300**, pp. 1269–1272 (2003).

2. Maryama, H. and Abbassi, A. "Comparative study of accurate experimentally determined and calculated band gap of amorphous ZnO layers", *Mater. Lett.*, **166**, pp. 206–209 (2016).

3. Ozgur, U., Alivov, Y.I., Liu, C., Teke, A., Reshchikov, M.A., Dogan, S., Avrutin, V., Cho, S.J., and Morkoc, H. "A comprehensive review of ZnO materials and devices", *J. Appl. Phys.*, **98**, pp. 11–1 (2005).

4. Purohit, A., Chander, S., Sharma, A., Nehra, S.P., and Dhaka, M.S. "Impact of low temperature annealing

on structural, optical, electrical and morphological properties of ZnO thin films grown by RF sputtering for photovoltaic applications", *Opt. Mater.*, **49**, pp. 51–58 (2015).

5. Fang, G., Li, D., and Yao, B.L. "Fabrication and vacuum annealing of transparent conductive AZO thin films prepared by DC magnetron sputtering", *Vacuum.*, **68**, pp. 363–372 (2002).
6. Ravichandran, K., Begum, N.J., Swaminathan, K., and Sakthivel, B. "Fabrication of a double layered FTO/AZO film structure having enhanced thermal, electrical and optical properties, as a substitute for ITO films", *Superlattices Microstruct.*, **64**, pp. 185–195 (2013).
7. Yan, X., Li, W., Aberle, A.G., and Venkataraj, S. "Textured AZO for Thin-Film Si Solar Cells: Towards understanding the effect of AZO film thickness on the surface texturing properties", *Procedia Engineering*, **139**, pp. 134–139 (2016).
8. Boujnah, M., Boumadyan, M., Naji, S., Benyoussef, A., Kenz, A.E., and Loulidi, M. "High efficiency of transmittance and electrical conductivity of V doped ZnO used in solar cells applications", *J. Alloy. Compd.*, **671**, pp. 560–565 (2016).
9. Suzuki, T. and Isoda, M. "Translucent material and method for manufacturing the same", CN 101006026 A (2007).
10. Rezaie, M.N., Manavizadeh, N., Abadi, E.M.N., Nadimi, E., and Boroumand, F.A. "Comparison study of transparent RF-sputtered ITO/AZO and ITO/ZnO bilayers for near UV-OLED applications", *Appl. Surf. Sci.*, **392**, pp. 549–556 (2017).
11. Lord, A.M., Maffeis, T.G., Allen, M.W., Morgan, D., Davies, P.R., Jones, D.R., Evansb, J.E., Smithe, N.A., and Wilkse, S.P. "Surface state modulation through wet chemical treatment as a route to controlling the electrical properties of ZnO nanowire arrays investigated with XPS", *Appl. Surf. Sci.*, **320**, pp. 664–669 (2014).
12. Chakraborty, M., Mahapatra, P., and Thangavel, R. "Structural, optical and electrochemical properties of Al and Cu co-doped ZnO nanorods synthesized by a hydrothermal method", *Thin Solid Films*, **612**, pp. 49–54 (2016).
13. Hao, X., Ma, J., Zhang, D., Yang, T., Ma, H., Yang, Y., and Huang, J. "Thickness dependence of structural, optical and electrical properties of ZnO:Al films prepared on flexible substrates", *Appl. Surf. Sci.*, **189**, pp. 137–142 (2002).
14. Zhang, L., Huang, J., Yang, J., Tang, K., Ren, B., Hu, Y., Wang, L., and Wang, L. "The effects of thickness on properties of B and Ga co-doped ZnO films grown by magnetron sputtering", *Mater. Sci. Semicond. Process*, **42**, pp. 277–282 (2016).
15. Liu, Y., Yang, S., Wei, G., Song, H., Cheng, C., Xue, C., and Yuan, Y. "Electrical and optical properties dependence on evolution of roughness and thickness of Ga:ZnO films on rough quartz substrates", *Surf. Coat. Technol.*, **205**, pp. 3530–3534 (2011).
16. Wang, Y., Lu, J., Bie, X., Gong, L., Li, X., Song, D., Zhao, X., Ye, W., and Ye, Z. "Transparent conductive Al-doped ZnO thin films grown at room temperature", *J. Vac. Sci. Technol. A*, **29**, pp. 031505 (2011).
17. Lee, H.W., Lau, S.P., Wang, Y.G., Tse, K.Y., Hng, H.H., and Tay, B.K. "Structural, electrical and optical properties of Al-doped ZnO thin films prepared by filtered cathodic vacuum arc technique", *J. Cryst. Growth*, **268**, pp. 596–601 (2004).
18. Liang, P., Cai, H., Yang, X., Li, H., Zhang, W., Xu, N., Li, H., Sun, J., and Wu, J.D. "Spectroscopic characterization of the plasmas formed during the deposition of ZnO and Al-doped ZnO films by plasma-assisted pulsed laser deposition", *Spectroc. Acta Pt. B-Atom. Spectr.*, **125**, pp. 18–24 (2016).
19. Suchea, M., Christoulakis, S., Katsarakis, N., Kitsopoulos, T., and Kiriakidis, G. "Comparative study of zinc oxide and aluminum doped zinc oxide transparent thin films grown by direct current magnetron sputtering", *Thin Solid Films*, **515**, pp. 6562–6566 (2007).
20. Fan, L. "The effect of thickness on electrical and optical properties of AZO films", *Journal of Ceramics*, **1**, pp. 23–26 (2015).
21. Zhou, H.M., Yi, D.Q., Yu, Z.M., Xiao, L.R., Li, J., and Wang, B. "Microstructure, optical and electrical properties of ZnO:Al prepared by sol-gel method", *Acta Metall. Sin.*, **5**, pp. 505–510 (2006).
22. Baskakov, I.V., Legname, G., Gryczynski, Z., and Prusiner, S.B. "Effect of the tungsten oxidation states in the thermal coloration and bleaching of amorphous WO3 films", *Thin Solid Films*, **384**, pp. 298–306 (2001).
23. Li, G., Wang, Z., Wang, Q., Wang, H., Du, J., Ma, Y., and He, J. "Effect of oxidation time under high magnetic field on the microstructure and optical properties of oxidized Co-doped ZnO films", *Acta Metall. Sin.*, **12**, pp. 1538–1542 (2014).
24. Yang, J., Wang, C., Tao, K., and Fan, Y. "A new method to obtain Cu films with lower resistivity and higher interface adhesion on different substrates", *J. Vac. Sci. Technol.*, **13**, pp. 481–484 (1995).
25. Haacke, G. "New figure of merit for transparent conductors", *J. Appl. Phys.*, **47**, pp. 4086–4089 (1976).
26. Wang, Q., Cao, Y., Li, G., Wang, K., Du, J., and He, J. "Improving the magnetic properties of molecular-beam-vapor-deposited Ni45Fe55 nanocrystalline films by in-situ high magnetic field application", *Sci. Adv. Mater.*, **5**, pp. 447–452 (2013).
27. Al-Ghamdi, A.A., Alhumminay, H., Abdel-Wahab, M.S., and Yahia, I.S. "Structure, optical constants and non-linear properties of high quality AZO nano-scale thin films", *Optik*, **127**, pp. 4324–4328 (2016).
28. Zhang, X., Chen, Y., Zhang, S., and Qiu, C. "High photocatalytic performance of high concentration Al-doped ZnO nanoparticles", *Sep. Purif. Technol.*, **172**, pp. 236–241 (2017).

29. Bahramian, R., Eshghi, H., and Moshaii, A. "Influence of annealing temperature on morphological, optical and UV detection properties of ZnO nanowires grown by chemical bath deposition", *Mater. Des.*, **107**, pp. 269–276 (2016).

30. Lin, Y.C., Jian, Y.C., and Jiang, J.H. "A study on the wet etching behavior of AZO (ZnO:Al) transparent conducting film", *Appl. Surf. Sci.*, **254**, pp. 2671–2677 (2008).

31. Zhong, Y., Ping, D., Song, X., and Yin, F. "Determination of grain size by XRD profile analysis and TEM counting in nano-structured Cu", *J. Alloy. Compd.*, **476**, pp. 113–117 (2009).

Biographies

Shiying Liu obtained her BEng degree from Dalian Jiaotong University in China in 2013 and her MEng with Professor Changbin Shen at the same university in 2016. She has been studying for her PhD in Prof. Qiang Wang's group at Northeastern University in China since September 2016.

Guojian Li obtained his PhD degree from the Northeastern University of China in 2009. He mainly studies the control of magnetic field in nanostructures and properties of low-dimensional materials. His main research fields are control of high magnetic field in the structure of functional film and its properties, structural design and functional composite of nano cutting coating under magnetic field, and multiscale simulation of nanostructure and properties under magnetic field. Professor Li has collaborated in 15 projects funded by the National Natural Science Foundation of China as well as some major national science and technology projects, in 10 of which he has been the principal investigator. He has published 68 papers of which 67 have been recorded by SCI and 17 are Q1 in JCR. These papers have been cited 221 times by SCI papers and in 36 cases, he is the first or corresponding author.

Lin Xiao obtained her BEng degree from Shenyang University of Technology in China in 2015 and has been an MEng student studying under Professor Guojian Li at the Northeastern University of China since September 2015.

Baohai Jia obtained his BEng degree from the Northeastern University of China in 2016 and has been an MEng student studying under Professor Guojian Li at the same university since September 2016.

Zhongyi Xu finished his graduation project in Professor Qiang Wang's group at the Northeastern University of China. He obtained his BEng degree in 2015.

Qiang Wang obtained his BEng and MEng degrees from the Northeastern University of China in 1995 and 1997, respectively, and his PhD from Nagoya University in Japan in March 2001. He was an Assistant Professor for two years at the Northeastern University of China and then, became a Professor and a doctorial tutor in 2003 and 2004, respectively. Professor Wang was an invited senior researcher in Materials Science and Engineering at University of California, Berkeley, in 2008.